



Theoretical Study of Fracture Toughness of Ceramic/Polymer Laminated Composites Using Cohesive Zone Simulations

N.A. Gadallah^{*}, R.M. Gadelrab[†], Y.E. Elshaer[‡], M.E. Abokhalaf[§]

Abstract: The fracture behavior of ceramic/polymer laminates has been investigated to improve fracture behavior of ceramic by reinforcing with ductile polymer layers. Epoxy is used to toughen ceramic laminates (partially stabilized Zirconia (PSZ) or Alumina). It is assumed that interface bonding between laminates takes place which was represented by cohesive zone model CZM. The ductile polymer layers are assumed ductile and cause bridging stress. A virtual model based on FEM is developed to calculate the J-integral of ceramic/polymer laminated composite numerically and as a mathematical expression for fracture toughness. The fracture toughness is studied by applying 3-point bend test on laminates. A parametric study of variables affecting J-integral is conducted. A verification of the finite element model has been performed by a comparison with previous research results which has been experimentally conducted by. A reasonable indication has been approved.

1. Introduction

With the increasing demands on multi-functional composites to resist wear, corrosion, thermal resistance and possess high toughness in mechanical, aerospace and biomedical applications, the development of multilayered material composites has come to the forefront. Traditional joining methods, e.g. welding, bolting, and riveting, cannot always be applied. Adhesive bonding is an alternative joining method that is widely used in the modern industry. The overall mechanical behaviour and response of layered composites depends on the mechanical properties and fracture/fatigue behaviour of the interfaces. The presence of interface between layers in ceramic composites provides preferential crack paths that enhance the overall fracture toughness of the composite [1]. Delamination may arise under various circumstances, such as low velocity impacts, or bearing loads in structural layers. The delamination failure mode is particularly important for the structural integrity of composite structures because it is difficult to detect during inspection [2].

2. Ceramic/Polymer Laminated Composite Materials

In the past years ceramic materials have become increasingly important especially for applications which require high-strength at elevated temperatures. The properties of the advanced ceramics are particularly attractive for structural applications primarily because of their excellent tribological properties such as in aerospace and biomedical fields, especially when the environmental conditions are particularly severe [3].

^{*} Professor, Modern Academy for Eng. & Tech, in Maadi, Cairo, Egypt.

[†] Professor, Dean of Elsalam Institute, Cairo, Egypt.

[‡] Egyptian Armed Forces, y_elsaer@hotmail.com

[§] Egyptian Armed Forces

The problem of using ceramic materials in construction is their brittle damage behaviour. Many techniques were used to improve the fracture toughness of the ceramics and in the present study, toughening was achieved by adding ductile polymer layers between ceramic layers.

3. Cohesive Zone Model CZM

Cohesive-zone models have been widely used in the last decades in many areas of fracture mechanics which deal with delamination, debonding and, more generally, with crack propagation and/or initiation at interface. CZM is used to represent the interface between layers. With respect to the conventional methods directly derived from fracture mechanics, the cohesive-zone models are generally preferred when structural behaviour is quasi brittle that is in presence of a non-negligible process zone on which the tractions more or less gradually decrease from a peak value to zero, or in conjunction with other types of material and geometrical non-linearity. Furthermore, they can be used for the analysis of crack initiation unlike fracture mechanics based techniques [4].

Cohesive damage zone models relate cohesive surface tractions, τ , to displacement jumps, Δ , at an interface where a crack may occur. Damage initiation is related to the interfacial strength, τ_0 , i.e., the maximum traction on the traction–displacement jump relation. The area under the traction–displacement jump relation is equal to the fracture toughness, G_c [2].

CZM has been used in the past to study crack tip plasticity and creep under static and fatigue loading conditions, crazing in polymers, adhesively bonded joints, interface cracks in bimetals, and crack bridging due to fibers and ductile particles in composites.

Interface modelling using CZM has the distinct advantage compared to other global approaches (e.g. shear lag model), in that it is based on a micro-mechanical approach. CZM was originally proposed by Barenblatt [5] as a possible alternative to the concept of fracture mechanics in perfectly brittle materials. Later, Dugdale [6] extended this concept to perfectly plastic materials by postulating the existence of a process zone at the crack tip.

CZM has spawned a plethora of models in fracture of metals, ceramics, and polymers and their composites [7-9]. Needleman is one of the first scientists who used polynomial and exponential types of traction–separation equations to simulate the particle debonding in metal matrices [10].

Xu and Needleman further used the above models to study the void nucleation at the interface between particle and matrix, fast crack growth in brittle materials under dynamic loading, and dynamic crack growth at the interface of bimetals. Tvergaard [11] used a quadratic traction–displacement jump form to analyze interfaces.

Tvergaard and Hutchinson [12] used a trapezoidal shape of the traction–separation model to calculate the crack growth resistance. Camacho and Ortiz [13] employed a linear traction–separation equation with an additional fracture criterion to propagate multiple cracks along arbitrary paths during impact damage in brittle materials.

Geubelle and Baylor [14] have utilized a bilinear CZM to simulate the spontaneous initiation and propagation of transverse matrix cracks and delamination fronts in thin composite plates subjected to low-velocity impact. In all the CZMs (except Dugdale's model and Camacho et al.'s model; see Table 1), the traction–separation relations for the interfaces are such that with increasing interfacial separation, the traction across the interface reaches a maximum, then decreases and eventually vanishes permitting a complete decohesion. The main difference lies in the shape and the constants that describe that shape.

Many researchers [15-17] have assumed that two independent parameters (cohesive energy and either of the cohesive strength or the separation displacement) are sufficient to model interfaces using CZM. Series of parametric studies indicate that this assumption leads to meaningless responses.

The responses clearly show (by the theory of contradiction) that those two parameters are not sufficient to represent the physics of the problem of the interface separation process. In order to accurately simulate the interface and reproduce the macroscopic mechanical behaviour of composites, CZM should include, apart from those two parameters, the shape of traction–separation law [18].

4. Finite Element Modelling of Laminated Ceramic/ Polymer

A simple model using FEM and based on (ANSYS 11) has been introduced in the present study. The ceramic/polymer laminated composite material is represented by a simple model shown in Fig. (1). Ceramic layers are the outer layers to provide environmental protection to the specimen. The thickness of polymer and ceramic layers are denoted by t_p and t_c respectively. A crack has been introduced in the layers to study the fracture behavior of the laminates. A number of intact polymer layers are used to study the polymer bridging stress. A three point bend loading is applied on the specimen.

Ceramic and polymer layers are represented by 2-D 4-Node Structural Solid element (plane182) in ANSYS software. CZM is used to describe the interface bonding between both ceramic and polymer layers and is represented by interface element (inter 202). The bridging stress caused by ductile polymer layers is represented in finite element model by nonlinear springs and they are introduced in ANSYS program as (COMBIN39).

Cohesive zone is defined by two parameters, Maximum normal traction at the interface, C1 and Normal separation at interface where maximum normal traction is attained, C2. The effect of these two parameters on laminates fracture toughness is studied and will be discussed later. A mapped meshing is used to mesh the model with 2D quadrilateral-shaped meshing element. The number of elements used was approximately 63,000 elements. To check the quality of this mesh, the number of elements has been increased 5 times and the difference in predicted maximum load to fracture was less than $\sim 0.6\%$, while the calculation time increased by about 10 times which means that mesh size does not have a strong effect on the accuracy of solution.

Only half of the specimen is used in solution to simplify analysis and to save computational time, symmetric conditions about Y-axis ($u_y = 0$ is applied after point of separation) is applied as shown in Fig. (2). A crack of length A is showed also. Fixed points are chosen at distance L_1 while the load is applied at the middle of the specimen (three point bend test).

Loading is applied between two values, minimum and maximum values P_{min} and P_{max} , an iteration method is used to solve the model and a measurement of stress in next ceramic layer, when stress in next ceramic layer equals ceramic fracture stress, a solution terminates. Finally J-integral is calculated as a measure of fracture toughness of ceramic/polymer laminated composite material. A flow chart describing the procedures to solve the problem is shown in Fig. (4).

Stress contours are obtained using the finite element model. Higher stresses are observed near the ceramic/polymer interface region and maximum stress was found in the next unbroken ceramic layer after crack tip, Fig. (3). Interface separation between bonded layers and represented by interface element (cohesive zone element) is shown in Fig. (5). Stress in next ceramic layer after crack tip increases to maximum value as shown in Fig. (6).

Crack opening displacement was measured by finite element at different crack lengths for different number of bridging layers, as shown in Fig. (7). A significant increase in crack opening displacement with the increase of bridging layers.

5. Effect of Different Laminate Parameters On Predicted J-Integral

5.1 Effect of Polymer Bridging Traction-Displacement $\sigma(U)$ Relation

Many researchers have studied the shape of traction-displacement function. Bannister and Ashby [19] have shifted the bridging stress-displacement relation, $\sigma(u)$ of ceramic/metal laminated composites to different values of peak stress and displacement according to degree of elasticity or strength of bonding between layers, Fig. (8).

Shifting of $\sigma_{br}(u)$ curve in the direction of constrained stress means bridging layer with higher strength, Fig. (9). While shifting of the curves in displacement direction means bridging layers more ductile Fig. (10). The effect of bridging layer mechanical properties on fracture toughness has been studied and it was found that stronger reinforcement causes higher fracture toughness specimens. Stronger reinforcement can prevent crack propagation and specimen needs to more energy to separate layers at the interface, Fig. (11).

Increasing the reinforcement plasticity leads to a decrease of fracture toughness, Fig. (12). Figure (13) represents the change of j-integral with ductility and strength of bridging layers. Increasing reinforcement ductility leads to reduction of fracture toughness of laminates while increasing of reinforcement strength increases fracture toughness of the laminates. At point of intersection of both curves a critical value of J-integral is obtained which is the optimum result of fracture toughness.

5.2 Effect of Laminate Geometry

Two parameters controlling the geometry were studied, the thickness ratio (t_p/t_c) and the number of laminates layers. For a constant layers number and the same specimen width, the J-integral curves were predicted for different thickness ratios.

The corresponding fracture toughness resistance curves are shown in Fig. (14). as expected, laminates with higher thickness ratio gives better toughening to the structure, for the same laminate width, W. Higher thickness ratio (t_p/t_c) means a thicker polymer layers which work as crack arresters and more stress is required to renucleate crack in next ceramic layer which leads to higher toughness. For the same thickness ratio, the effect of number of layers on the fracture toughness is shown in Fig. (15). The smaller number of layers in the laminates leads to higher thickness of the polymer and ceramic layer leading to an increase of fracture toughness.

The critical load for crack propagation was studied as well to inspect the effect of geometrical parameters on the crack growth stability within the laminate. Increasing number of layers causes an increase in critical load to fracture until certain value then loads begins to decrease significantly. This means that an optimization design is required to get the best toughness design for the specimens.

5.3 Effect of Ceramic Properties

The effect of ceramic modulus of elasticity on the fracture toughness of the specimens has been studied; three different values of ceramic stiffness were used, 195, 385 and 770 GPa. Increasing ceramic stiffness from 192 [GPa] to 385 [GPa] leads to an increase of fracture toughness from 0.148 to 0.3 [kJ/m²]. That means that the increase in ceramic stiffness leads to an equivalent increase of fracture toughness with about the same ratio of stiffness increase. Increasing the ceramic stiffness to higher values 770 [GPa] causes an intensive increase in laminate toughness that is an increase from 385 to 770 GPa means causes a fracture toughness increase by 0.3 to 1.9 [kJ/m²].

5.4. Effect of Polymer Properties

Different values of polymer stiffness were studied, (100 MPa, 200MPa, 300MPa and 400MPa). There was no significant effect for polymers modulus of elasticity on toughness of laminates and the variation of j-integral with polymer elasticity is very small in comparison to the effect of ceramic modulus of elasticity. The reason is the elastic mismatch.

5.5 Effect of Interface Properties between Ceramic and Polymer Layers

Three cohesive zone parameters are used to define the interface between ceramic and polymer namely, C_1 , C_2 and C_3 . C_1 is the maximum normal traction at interface; C_2 is Normal separation at interface where maximum normal traction is attained and C_3 is Shear separation where the maximum shear traction is attained. In the present study, the effect of C_1 and C_2 on fracture toughness and critical load is studied. As C_1 increases, critical load to fracture increases due to the increase of normal stress that the interface can support, Fig. (19). Crack growth can occur at the beginning after maximum cohesive energy is absorbed then the interface will support no load after this point. Fracture toughness curve accordingly was classified into three regions. The first zone showed very small reducing in toughness curve with increasing C_1 then the second region in Fig.(20) is a rapid increase in fracture toughness with caused by amount of high energy absorbed to break the cohesive forces at interface according to high values of interface normal stress. The third region showed a decrease in fracture toughness after fiber breakage.

Figure (21) and (22) show the effect of C_2 on critical load and J-integral. The two curves show an increase of both critical load and fracture toughness of specimen with increasing C_2 . Increasing C_2 means that more loading is required to initiate crack at next ceramic layer and to separate layers from each other, this means more energy is required to separate them.

6. Verification of Finite Element Model

In order to verify the results of the presented theoretical work based on finite element model and check its accuracy, the results have been compared to previous research results by J.K. Spelt et al. [20] who proposed an experimental method to determine the J-R curve behavior for two different rubber-toughened epoxy adhesives with AA6061-T6 aluminium DCB adherends as a function of the mode ratio [21]. ANSYS ver. 11 has been used to model the adherend and the adhesive material. Cohesive zone elements (inter 202) with mode I exponential traction – separation law were used with 2D structural solid elements (PLANE 182).

Load vs. crosshead displacement at the point of applying load were calculated by the FEM and were compared with the experimental results. Figure (23) shows experimental results for load-displacement curves calculated at different crack lengths varying from 80.6 mm to 115.4 mm and a comparison with results obtained for each case and calculated by FEM showed good coincidences. Appendix (2B) represents the FEM used to verify the experimental results.

Strain energy release rate was calculated by J.K. Spelt et Al. [20] using the three methods prescribed by British Standard BS7991:2001 [22]. The simple beam theory (SBT), corrected beam theory (CBT), and experimental compliance method (ECM) gave very similar results.

G_{cs} values calculated by the four methods already mentioned were compared with FEM results. Good result can be observed as shown in Fig. (24). Simple beam theory (SBR) experimental results gave very close results to finite element results with an error 1.49 %, while beam on elastic foundation (BOEF) was the biggest error from finite element results with an error 10% Compact beam theory (CBT) and experimental compliance method (ECM) gave similar results with error 6.6% and 6.3% respectively.

7. Conclusion

In the present study, fracture toughness of ceramic/polymer laminated composites has been studied. The specimens were subjected to three point loading and J-integral was calculated as a mathematical expression for fracture toughness. The interface between ceramic and polymer layers is represented by cohesive zone model. A finite element model is proposed to calculate fracture toughness. The effect of different parameters of fracture toughness is studied and it was found that increasing polymer layer thickness (by increasing thickness ratio) improves the fracture toughness behavior of laminates. The variation of polymer and ceramic modulus of elasticity and interface between ceramic and polymer layers and constrained polymer have been examined to check their effect on fracture toughness of the materials. Ceramic modulus of elasticity showed significant effect on fracture toughness of the specimens on the contrary of polymer modulus of elasticity which did not give significant effect due to elastic mismatch. Increasing the cohesive zone parameters improved specimen fracture toughness. Polymer bridging constraints are varied by changing the peak values of stress and strain values. The results show that it is preferable to use bridging layers with higher strength and less plasticity properties.

References.

- [1] N. Sukumar, Z. Huang, J. Prévost and Z. Suo, "Partition of Unity Enrichment for Bimaterial Interface Cracks", International journal for numerical methods in engineering, Part 59, pp.1075–1102, (2004).
- [2] A. Turon, C.G. Dávila, P.P. Camanho, J. Costa, "An engineering solution for mesh size effects in the simulation of delamination using cohesive zone models", Engineering Fracture Mechanics, part 74, pp. 1665–1682, (2006).
- [3] G. Stantshev, M. Friea, R. Kochendörfer, W. Krenkelb, "Long fiber reinforced ceramics with active fillers and a modified intra-matrix bond based on the LPI process", Germany Journal of the European Ceramic Society, Part 25, pp. 205–209, (2005).
- [4] G. Alfano, "On the influence of the shape of the interface law on the application of cohesive-zone models", Composites Science and Technology, Part 66, pp. 723–730, (2006).
- [5] G. I. Barenblatt, "The formation of equilibrium cracks during brittle fracture", General ideas and hypothesis. Axially-symmetric cracks. Prikl. Matem. I mekham, Part 23, pp. 434–444, (1959).
- [6] D. S. Dugdale, "Yielding of steel sheets containing slits", Journal of the Mechanics and Physics of Solids, Part 8, pp. 100–104, (1960).
- [7] A. Needleman, "An analysis of tensile decohesion along an interface", Journal of the Mechanics and Physics of Solids, Part 38, pp. 289–324, (1990) a.
- [8] A. Needleman, "An analysis of decohesion along an imperfect interface", International Journal of Fracture, Part 42, pp. 21–40, (1990) b.
- [9] D. Wappling, J. Gunnars, P. Stahle, "Crack growth across a strength mismatched bimaterial interface", International Journal of Fracture, Part 89, pp. 223–243, (1998).
- [10] A. Needleman, "Numerical modeling of crack growth under dynamic loading conditions", Computational Mechanics, Part.19 (6), pp. 463–469, (1997).
- [11] V. Tvergaard, "Effect of fiber debonding in a whisker-reinforced metal", Material Science and Engineering, Part 125 (2), pp. 203–213, (1990).
- [12] V. Tvergaard, J.W. Hutchinson, "The relation between crack growth resistance and fracture process parameters in elastic–plastic solids", Journal of the Mechanics and Physics of Solids, Part 40 (6), pp. 1377–1397, (1992).
- [13] G.T.Camacho, M. Ortiz, "Computational modeling of impact damage in brittle materials", International Journal of Solids and Structures, Part 33, pp. 2899–2938, (1996).
- [14] P.H. Geubelle, J. Baylor, "Impact-induced delamination of laminated composites: a 2D simulation", Composites Part B Engineering, Part 29(5), 589–602, (1998).

- [15] N. Chandra, H. Li, C. Shet, H. Ghonem, "Some issues in the application of cohesive zone models for metal–ceramic interfaces", *International Journal of Solids and Structures*, Part 39, pp. 2827–2855, (2002).
- [16] P. Rahulkumar, A. Jagota, S.J. Bennison, "Cohesive element modeling of viscoelastic fracture: application to peel testing of polymers", *International Journal of Solids and Structures*, Part 37, pp. 1873–1897, (2000).
- [17] I. Mohammed, K.M. Liechti, "Cohesive zone modeling of crack nucleation at bimaterial corners", *Journal of the Mechanics and Physics of Solids*, Part 48, pp. 735–764, (2000).
- [18] J.W. Hutchinson, A.G. Evans, "Mechanics of materials: top-down approaches to fracture", *Acta Materialia*, Part 48 (1), pp. 125–135, (2000).
- [19] M. Bannister, M. F. Ashby, "The deformation and fracture of constrained metal sheets", *Acta Metall. Mater.*, Part 39(11), pp. 2575-2582, (1991).
- [20] A. Ameli, M. Papini, J.A. Schroeder, J.K. Spelt, "Fracture R-curve characterization of toughened epoxy adhesives", *Engineering fracture mechanics*, Part 77, pp. 521–534, (2010).
- [21] G. Fernlund, J.K. Spelt, "Mixed-mode fracture characterization of adhesive joints", *Composite Science Technology*, Volume 50, pp. 441–449. (1994).
- [22] BSI. Determination of the mode I adhesive fracture energy, GIC, of structural adhesives using the double cantilever beam (DCB) and tapered double cantilever beam (TDCB) specimens; BS 7991: 2001.

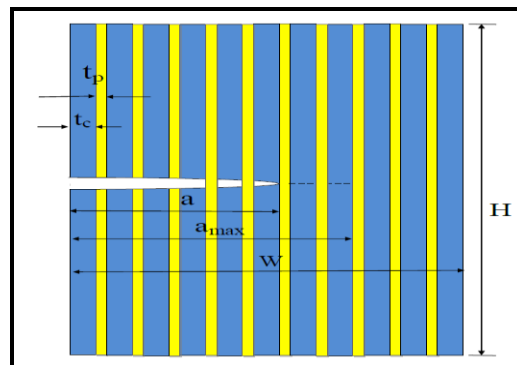


Fig. (1) A simple model for ceramic/polymer laminated composite material.

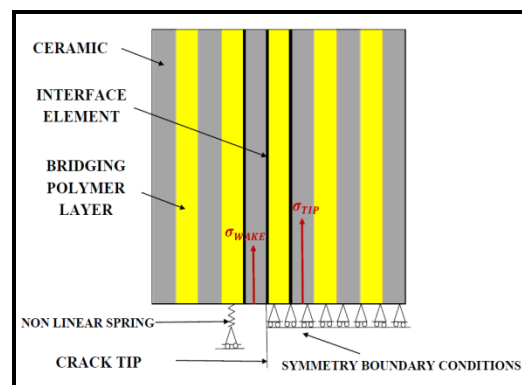


Fig. (2) Finite element model used to study the fracture toughness of ceramic/polymer laminate composites.

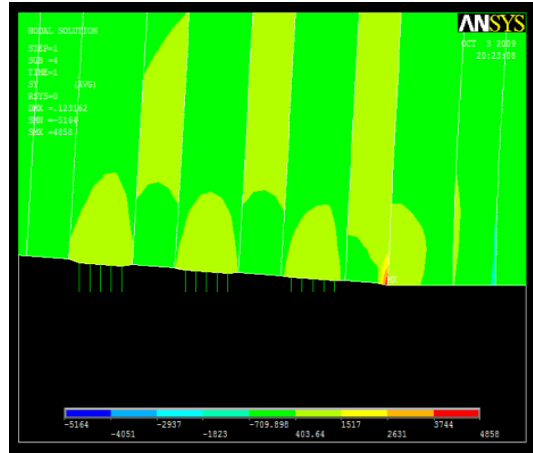


Fig. (3) Stress distribution in a ceramic/polymer laminate using FEM.

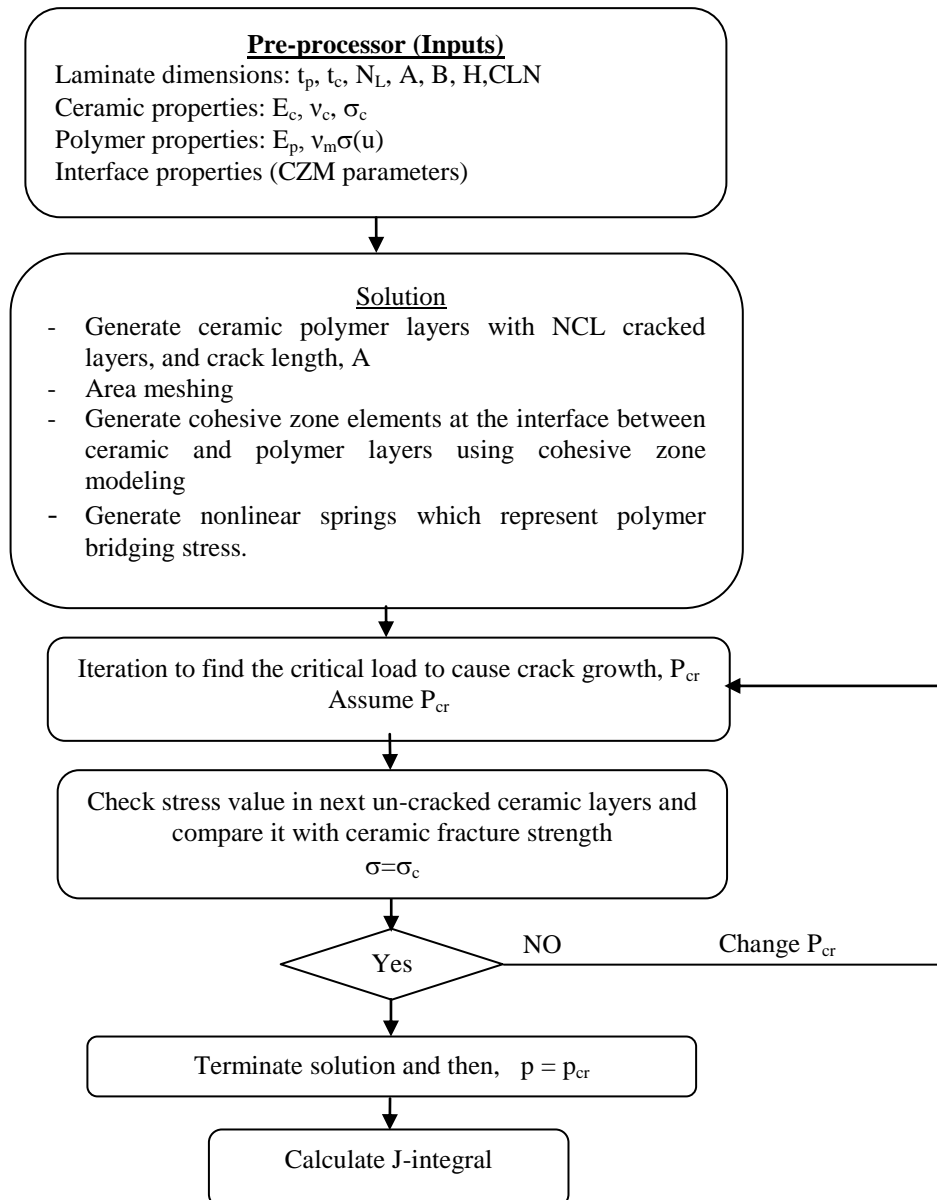


Fig. (4) Block diagram of modeling J-integral using FEM by ANSYS.

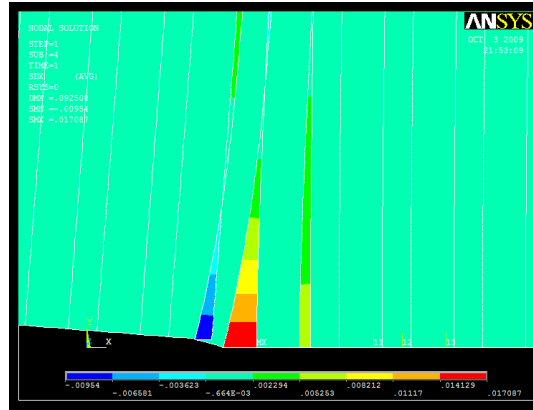


Fig. (5) X-component of interface separation between ceramic and polymer interface layers at crack tip.

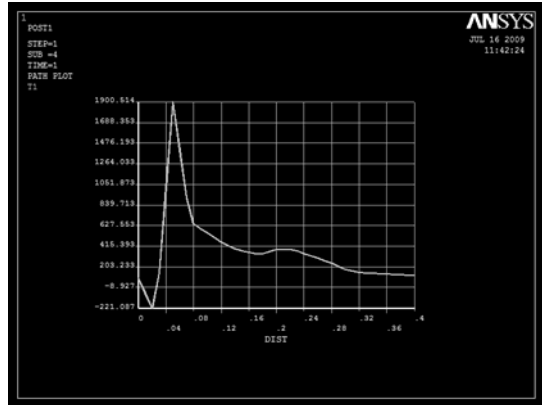


Fig. (6) Stress distribution along next unbroken ceramic layer (σ_{tip}).

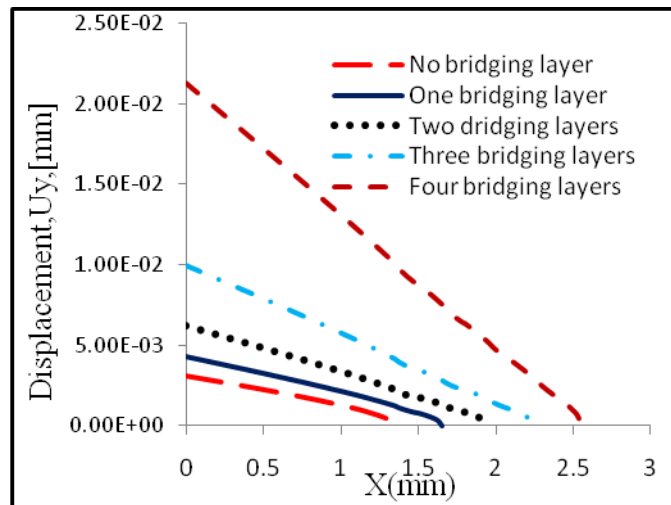


Fig. (7) Predicted COD by FEM for different crack size.

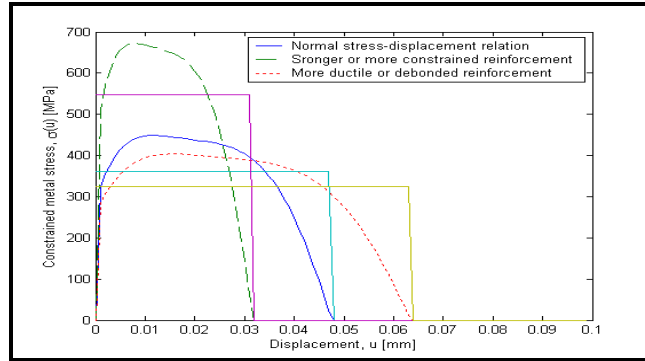


Fig. (8) Different bridging constraints relations, and the corresponding rectilinear representation [19].

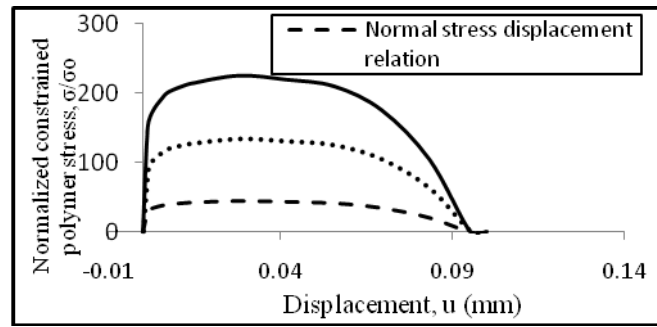


Fig. (9) Different strength values for constrained polymer stress.

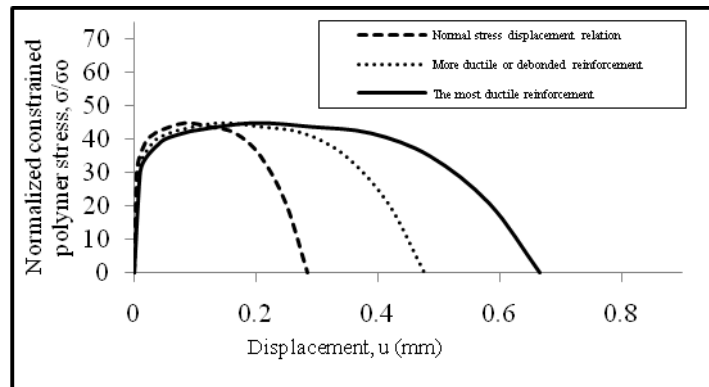


Fig. (10) Different ductility values for constrained polymer stress.

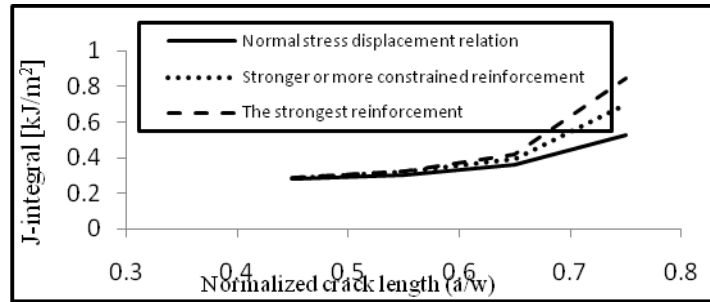


Fig. (11) J-R curves for different strength reinforcements.

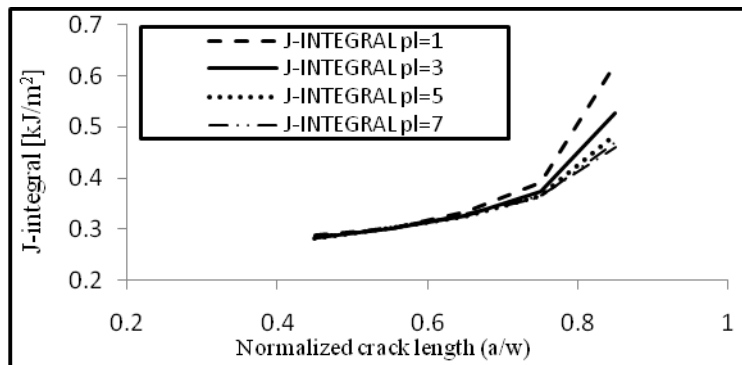


Fig. (12) Effect of reinforcement plasticity on J-R curves (PL represents degree of ductility, higher PL means higher ductility).

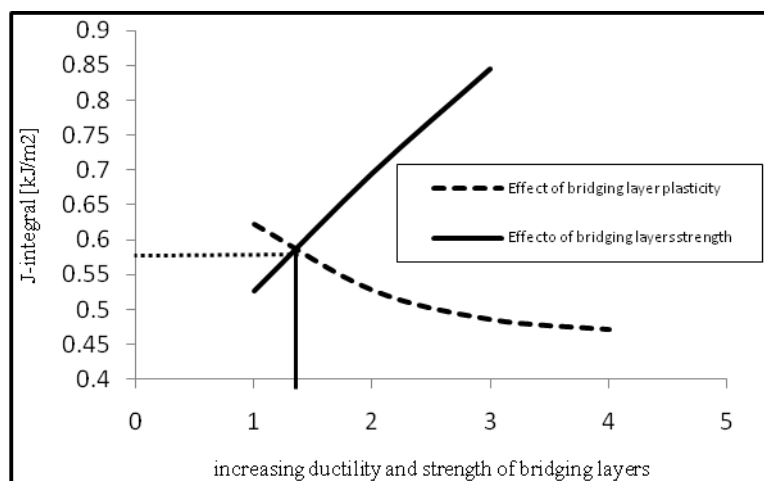


Fig. (13) J-integral as a function of ductility and strength of bridging reinforcement layers.

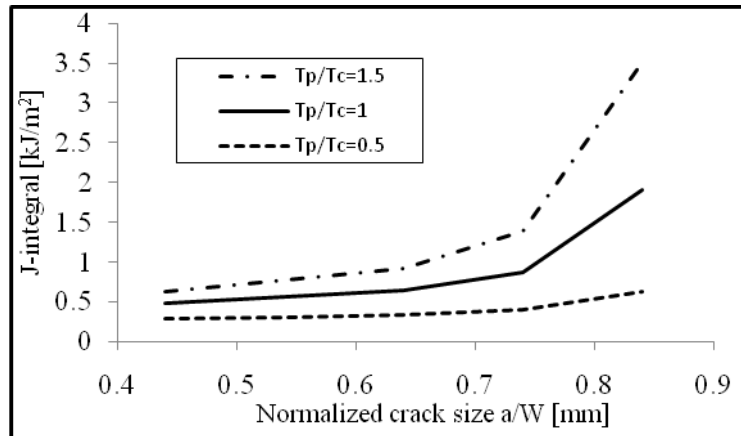


Fig. (14) Effect of thickness ratio on the J-R curves (NCL=11, W=3.1mm)

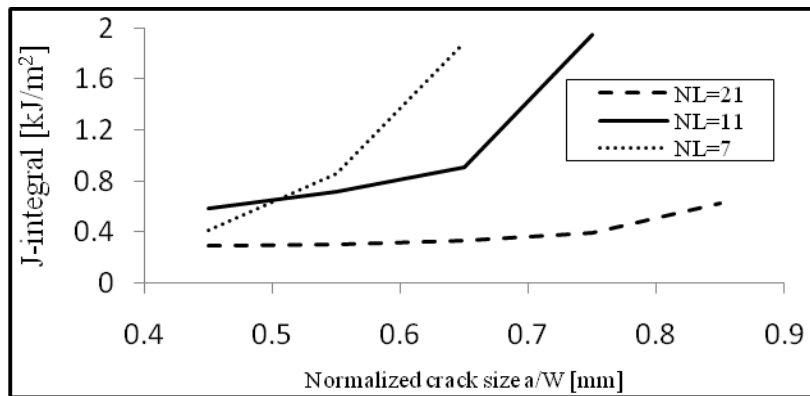


Fig. (15) Effect of number of layers on the J-R curves (Tp/tc=0.5 W=3.2).

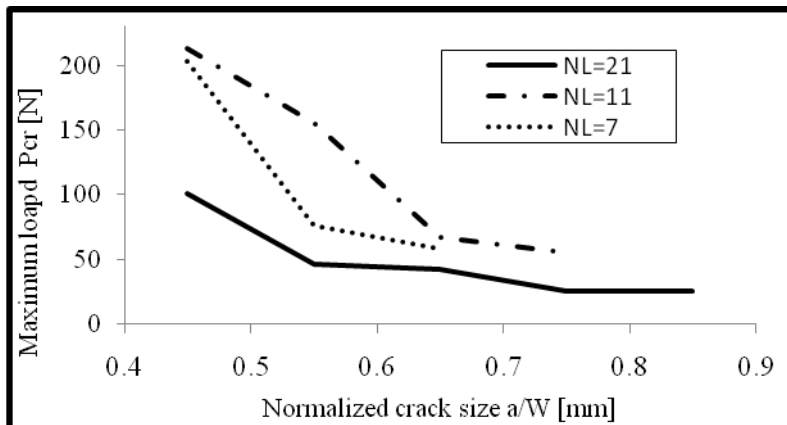


Fig. (16) Effect of number of layers on the critical load for crack propagation (tp/tc=0.5 W=3.2).

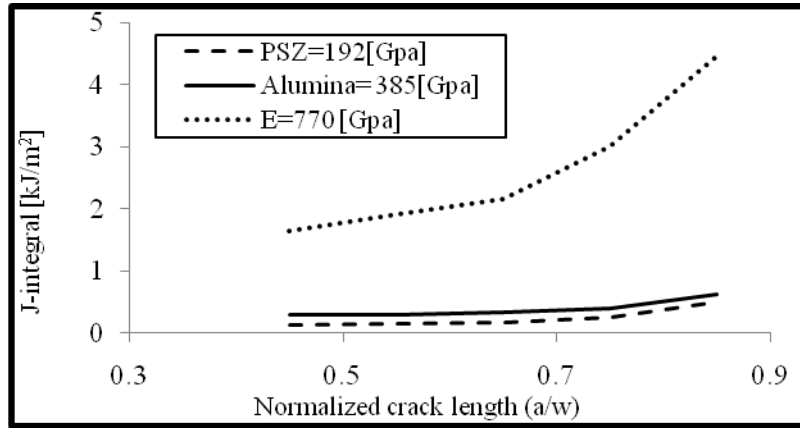


Fig. (17) Effect of ceramic stiffness on J-R curves.

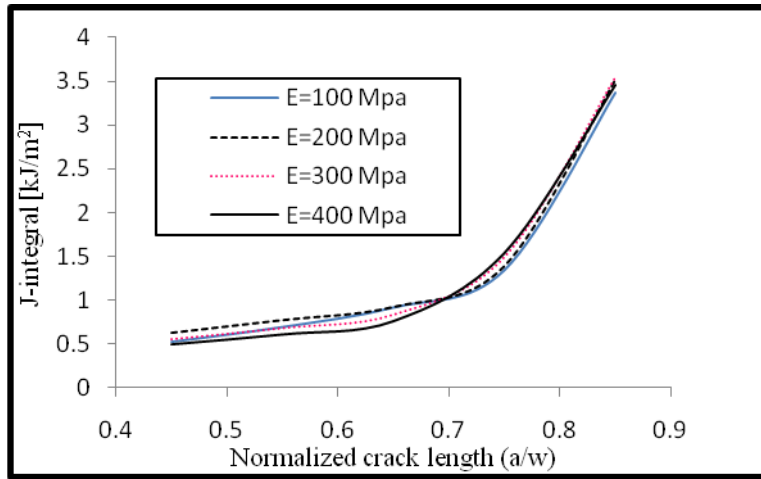


Fig. (18) Effect of polymer modulus of elasticity on J-R curves.

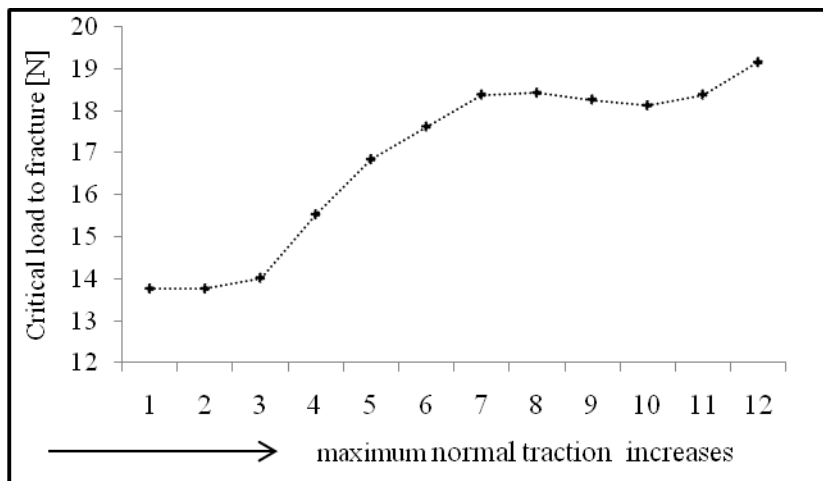


Fig. (19) Effect of maximum normal traction at the interface C₁ on critical load to fracture.

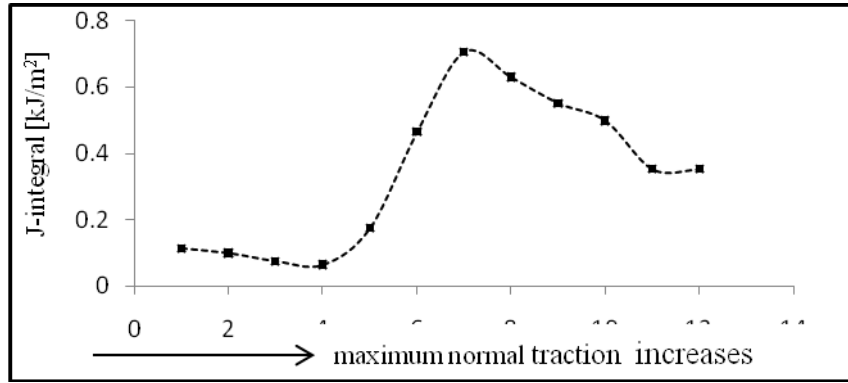


Fig. (20) Effect of maximum normal traction at the interface C_1 on J-integral.

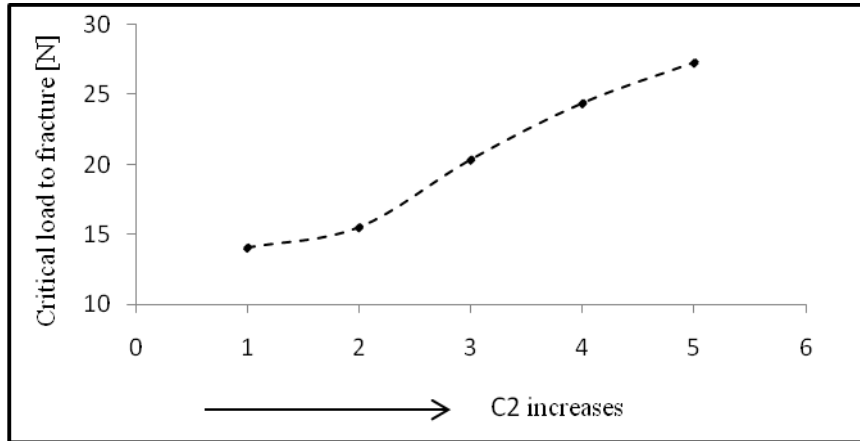


Fig. (21) Effect normal separation across the interface where the maximum normal traction is attained C_2 on critical load to fracture.

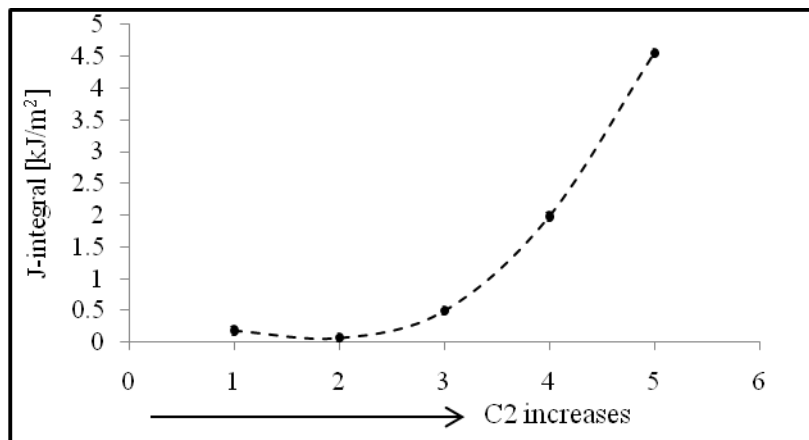


Fig. (22) Effect of normal separation across the interface (C_2) on J-integral.

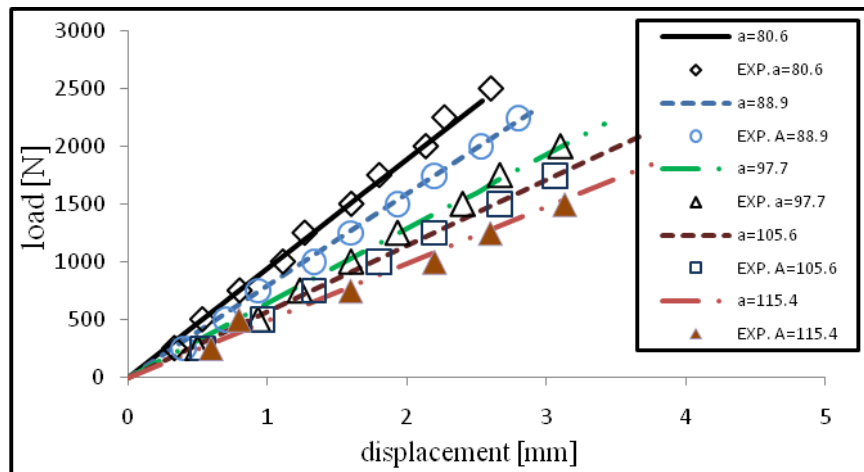


Fig. (23) A comparison between experimental results obtained from [92] and present FEM output results for load vs. crosshead displacement at the applying load point.

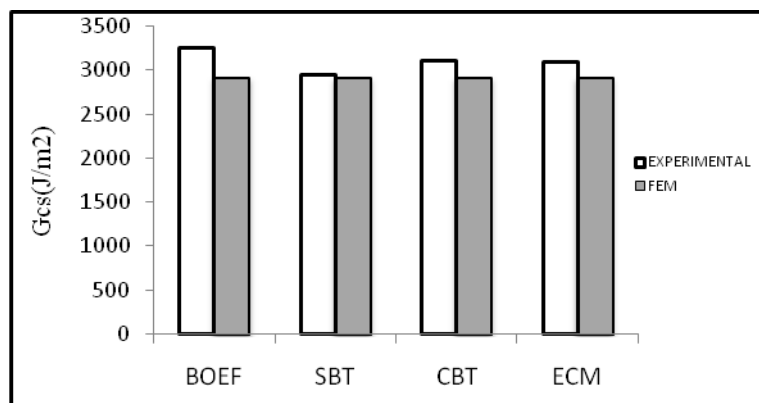


Fig. (24) Strain energy release rate in mode I calculated by the FEM and different experimental methods.